On the evolution of the solar wind between 1 and 5 AU at the time of the Cassini Jupiter flyby: Multispacecraft observations of interplanetary coronal mass ejections including the formation of a merged interaction region

P. G. Hanlon,[1] M. K. Dougherty,[1] R. J. Forsyth,[1] M. J. Owens,[1] K. C. Hansen,[2] G. Tóth,[3] F. J. Crary,[4] and D. T. Young[4]

Received 30 June 2003; revised 3 December 2003; accepted 19 December 2003; published 29 June 2004.

[1] The Cassini flyby of Jupiter occurred at a time near solar maximum. Consequently, the pre-Jupiter data set reveals clear and numerous transient perturbations to the Parker Spiral solar wind structure. Limited plasma data are available at Cassini for this period due to pointing restrictions imposed on the instrument. This renders the identification of the nature of such structures ambiguous, as determinations based on the magnetic field data alone are unreliable. However, a fortuitous alignment of the planets during this encounter allowed us to trace these structures back to those observed previously by the Wind spacecraft near the Earth. Of the phenomena that we are satisfactorily able to trace back to their manifestation at 1 AU, two are identified as being due to interplanetary coronal mass ejections. One event at Cassini is shown to be a merged interaction region, which is formed from the compression of a magnetic cloud by two anomalously fast solar wind streams. The flux-rope structure associated with this magnetic cloud is not as apparent at Cassini and has most likely been compressed and deformed. Confirmation of the validity of the ballistic projections used here is provided by results obtained from a one-dimensional magnetohydrodynamic projection of solar wind parameters measured upstream near the Earth. It is found that when the Earth and Cassini are within a few tens of degrees in heliospheric longitude, the results of this one-dimensional model predict the actual conditions measured at 5 AU to an impressive degree. Finally, the validity of the use of such one-dimensional projections in obtaining quasi-solar wind parameters at the outer planets is discussed. *INDEX TERMS:* 7513 Solar Physics, Astrophysics, and Astronomy: Coronal mass ejections; 2111 Interplanetary Physics: Ejecta, driver gases, and magnetic clouds; 2134 Interplanetary Physics: Interplanetary magnetic fields; 2139 Interplanetary Physics: Interplanetary shocks; 2164 Interplanetary Physics: Solar wind plasma; *KEYWORDS:* solar wind, merged interaction region, Cassini, MHD propagation

Citation: Hanlon, P. G., M. K. Dougherty, R. J. Forsyth, M. J. Owens, K. C. Hansen, G. Tóth, F. J. Crary, and D. T. Young (2004), On the evolution of the solar wind between 1 and 5 AU at the time of the Cassini Jupiter flyby: Multispacecraft observations of interplanetary coronal mass ejections including the formation of a merged interaction region, *J. Geophys. Res.*, *109*, A09S03, doi:10.1029/2003JA010112.

1. Introduction

[2] The Cassini spacecraft was launched on 15 October 1997, beginning its 7-year journey to Saturn. One of the largest and most sophisticated interplanetary spacecraft ever constructed, it carries with it not only a wealth of scientific instruments that will enable both remote and in situ measurements of the Saturnian system but also the Huygens probe that will be deployed into the atmosphere of the moon Titan. En route to Saturn, the Cassini spacecraft passed by the boundaries of the Jovian magnetic environment. Closest approach to the planet took place on 30 December 2000, at a distance of 138 R_J on the duskside.

[3] The main science objectives of this flyby were to gain an understanding of the solar wind influence on the Jovian system. This was possible due to the unique combined data sets taken by Cassini and the orbiting Galileo spacecraft [e.g., *Gurnett et al.*, 2002; *Hanlon et al.*, 2004]. In addition, observations from the Hubble Space Telescope (HST) of Jupiter's auroral emissions are available for this period [*Clarke et al.*, 2002].

[1]Space and Atmospheric Physics Group, Blackett Laboratory, Imperial College London, London, UK.
[2]Department of Atmospheric, Oceanic, and Space Sciences, University of Michigan, Ann Arbor, Michigan, USA.
[3]Department of Atomic Physics, Loránd Eötvös University, Budapest, Hungary.
[4]Southwest Research Institute, San Antonio, Texas, USA.

0148-0227/04/2003JA010112$09.00

[4] This paper will be concerned with the upstream solar wind observations taken by the Cassini spacecraft during the few months preceding closest approach. The magnetic field data set reveals many transient perturbations to the Parker spiral during Cassini's approach to Jupiter. These structures are shown to be linked to observations taken upstream near the Earth, which was within a few tens of degrees of Jupiter in heliospheric longitude. One of these large magnetic field perturbations observed by Cassini is shown to be a merged interaction region, formed by the compression of a magnetic cloud by two anomalously fast solar wind streams.

2. Coronal Mass Ejections and Merged Interaction Regions

[5] Coronal mass ejections (CMEs) are large eruptions of solar material into interplanetary space [e.g., *Hundhausen*, 1993; *Cargill*, 2001]. Once ejected from the Sun, their interplanetary counterparts (ICMEs) constitute transient solar wind streams as their speed, temperature [*Gosling et al.*, 1973; *Richardson and Cane*, 1995], p^+ to He^{++} ratio [*Borrini et al.*, 1982], charge state composition [*Lepri et al.*, 2001; *Henke et al.*, 2001], and magnetic field structure can differ greatly from that of the ambient medium [*Gosling*, 1990; *Neugebauer and Goldstein*, 1997].

[6] Magnetic clouds (MCs) are a subset of ICMEs observed in spacecraft data. MCs are often defined as an ICME that has a smooth rotation in the magnetic field direction, an overall accompanying increase in the field magnitude, and a low proton temperature [*Burlaga et al.*, 1981; *Klein and Burlaga*, 1982]. This magnetic field rotation is thought to be due to a flux rope structure convecting over the spacecraft [*Burlaga*, 1998; *Lepping et al.*, 1990].

[7] ICMEs can have a high velocity in the solar wind rest frame [e.g., *Gopalswamy et al.*, 2001]. Consequently, compression of the downstream solar wind frequently causes the leading edges of ICMEs to be preceded by a region of increased magnetic field magnitude, particle density, and temperature. This is termed the sheath or "pile-up region." Frequently, the leading edge of an ICME is observed to be moving faster than its trailing edge; this is due to the structure expanding in the radial direction as it as it travels antisunward. A shock wave will develop on the leading edge of an ICME if it is moving in the solar wind frame with a velocity greater than that of the fast-mode magnetosonic speed.

[8] Merged interaction regions (MIRs) are defined as the structure resulting from the interaction and coalescence of two or more transient solar wind events. MIRs are generally split into three categories: corotating (CMIRs), local (LMIRs), and global (GMIRs), [*Burlaga and Ness*, 1993]. Generally, an MIR is formed when the forwardly moving edge of a faster event encounters the rear end of a slower leading event, with interactions taking place between the two original events, forming one larger overall structure [*Burlaga*, 1995, and references therein].

[9] Previous investigations into the evolution of ICMEs within the solar wind have been undertaken [*Paularena et al.*, 2001; *Wang et al.*, 2001; *Richardson et al.*, 2002]. *Paularena et al.* [2001] presented an interconnected series of observations of ICMEs from 5 to 58 AU, showing that He^{++}/p^+ enhancements can be used to track such structures to the outer heliosphere. *Richardson et al.* [2002] presented follow-up observations (and MHD modeling), which showed an MIR at 58 AU that was formed by the compression of multiple ICMEs observed upstream. These observations, however, were highly longitudinally separated. Here we outline dual spacecraft observations of solar wind structures at 1 and 5 AU, where the longitudinal separation between the spacecraft was less than a few tens of degrees.

3. Observations

[10] Figure 1 shows 27-day solar rotation summary plots of the Cassini fluxgate magnetometer data [*Dougherty et al.*, 2004] from DOY (day of year) 2000-276 to DOY 2001-031. This period incorporates the upstream observations, closest approach on DOY 2000-365, as well as the entry of the spacecraft into the Jovian magnetosheath and magnetosphere (described in further detail by M. K. Dougherty et al. (Cassini's view of Jupiter's magnetic environment, submitted to *Journal of Geophysical Research*, 2004, hereinafter referred to as Dougherty et al., submitted manuscript, 2004)). In each of the four panels of the figure, the upper section shows the magnetic field magnitude and the lower section shows the φ angular direction of the field measured in the standard RTN sense (with R pointing radially away from the Sun toward the spacecraft, N being defined by the vector R and the solar rotation axis, and T making a right-handed set; φ is then the angle in the R-T plane with 0 degrees defined as along R away from the Sun, increasing in a right-handed sense). This angular view of the magnetic field allows crossings of the heliospheric current sheet (HCS) to be clearly observed by abrupt approximately 180° changes in the field direction.

[11] It can clearly be seen in all panels that the field magnitude can be separated into two basic categories; an undisturbed solar wind with a magnitude of approximately 0.3 nT and the many clear transient enhancements, which can reach as high as 4 nT. It is these transient enhancements that this paper will be concerned with.

3.1. DOY 2000-323 Event

[12] Let us initially turn our attention to the structure starting DOY 2000-323 at 1700 UT, clearly seen in Figure 1 but also shown in more detail in Figure 2. This figure shows in addition to the field magnitude and φ angle, the θ angle (measured from the R-T plane, positive in the N direction) and the solar wind velocity as measured by the Cassini Plasma Spectrometer (CAPS) Ion Beam Spectrometer (IBS) instrument in the bottom panel [*Young et al.*, 2004] (measured by fitting Maxwellian distributions to the observed energy spectra). The large gaps seen in these data resulted from the instrument being unable to view in the direction of the solar wind flow continuously throughout the period in question. This was due to pointing restrictions that were imposed upon the spacecraft by a scheduled remote sensing campaign.

[13] The onset of the event is marked by a sharp discontinuity in the field magnitude, indicative of a forwardly propagating shock wave. The trailing edge of the structure is marked by a steep return to the ambient solar wind conditions. Although not apparent at the scale plotted on Figure 2, the gradient of this reverse wave is significantly less than that of the initial forwardly propagating shock.

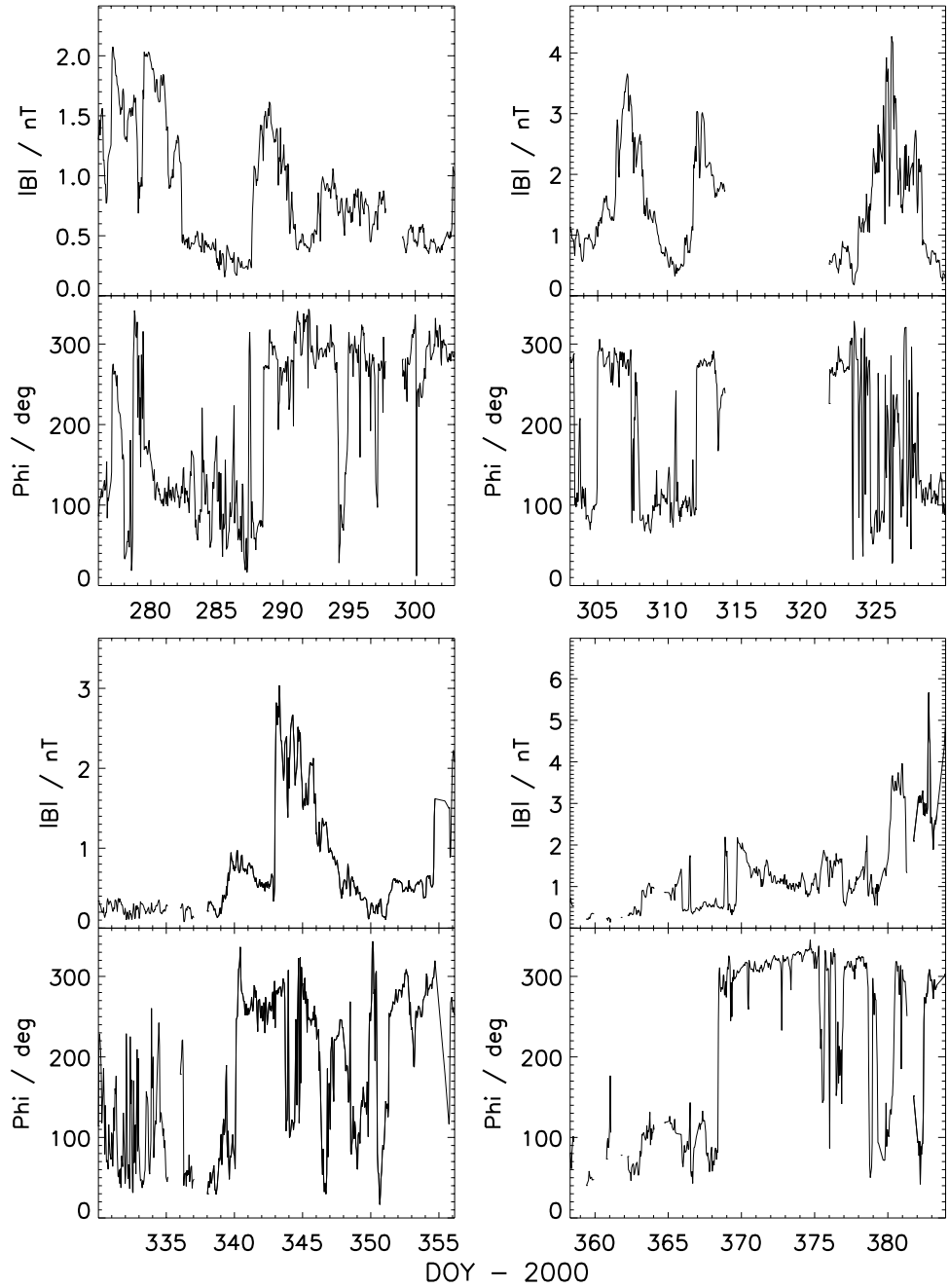

Figure 1. Twenty-seven day summary plots of the pre-Jupiter Cassini Dual Technique Magnetometer (MAG) data, showing the magnetic field magnitude and the φ angle (defined in text). Abrupt 180-degree flips in the φ angle indicate crossings of the heliospheric current sheet (HCS).

This may be a reverse shock wave; however, determinations are hindered by the lack of continuous plasma data.

[14] Under ambient solar wind conditions, the φ angle at this heliospheric distance would be expected to lie in the Parker Spiral direction, either at $\sim$120° or $\sim$300°, depending on which side of the HCS the spacecraft was currently on. It can clearly be seen in Figure 2 that the Parker Spiral configuration dominates both before ($\varphi \sim 300°$) and after ($\varphi \sim 120°$) the event, with a current sheet crossing hence occurring some time during the event itself. Although within the event the φ angle is highly disturbed, the current sheet crossing, which takes the magnetic field from being on average one polarity to being the other, can be seen to occur approximately half way through DOY 324.

[15] This particular solar wind event has been previously mentioned in relationship to a large enhancement in the Jovian hectometric radio emissions as observed by the Cassini Radio and Plasma Wave Science (RPWS) [*Gurnett et al.*, 2004] and Galileo Plasma Wave Science (PWS) [*Gurnett et al.*, 1992] instruments [*Gurnett et al.*, 2002]. In addition it has also been associated with a large increase in the FUV aurora at Saturn [*Prangé and Pallier*, 2002],

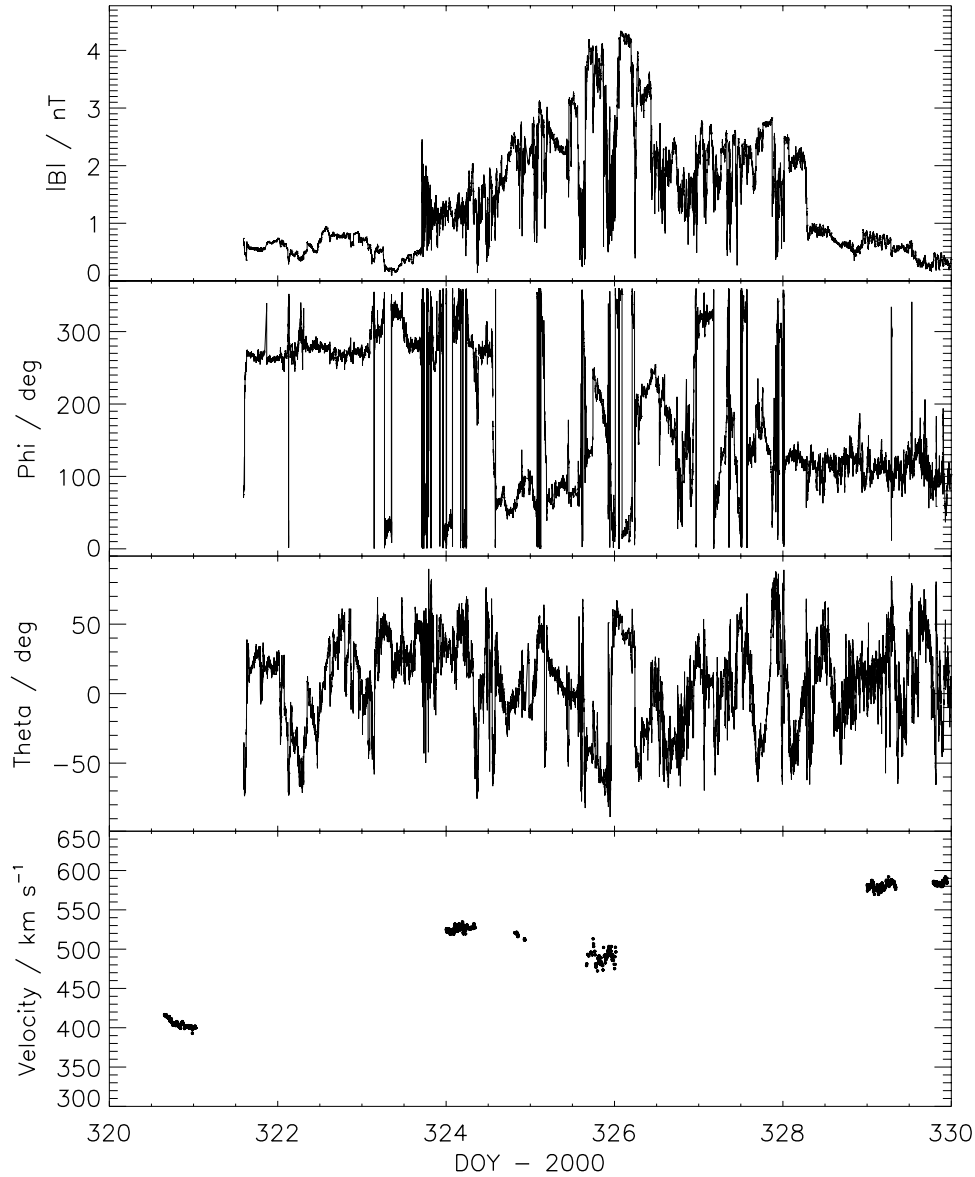

Figure 2. The DOY 323–328 solar wind event observed by Cassini. Plotted are the magnetic field magnitude, the φ and θ angles (defined in text), and the solar wind velocity in the antisunward direction as measured by the Center for Analysis and Prediction of Storms (CAPS) Ion Beam Spectrometer (IBS) instrument. The sparse data coverage in the bottom panel is due to the instrument not being able to point continuously in the solar wind flow due to scheduled remote sensing operations.

which was also within a few tens of degrees in heliospheric longitude during this period.

3.2. Correlation Between Cassini and Wind

[16] At this point we will note that the Earth and Cassini were very well radially aligned during this period. The difference in latitude between the Earth and Cassini was never greater than 3° throughout the data set. Longitudinal opposition occurred late on DOY 335, with the relative angular velocity between the two planets altering the angle by just less than 1 degree per day. This leads us to consider the possibility that the DOY 323 structure observed by Cassini (Figure 2) could be correlated with observations taken upstream near the Earth.

[17] In order to search for such possible correlations, the Wind magnetic field and plasma data were investigated. Wind makes highly eccentric Earth orbits that take it out into the solar wind and allow it to take in situ measurements of the interplanetary medium. For the period in question, Wind was sunward of the magnetosphere, far out on the dawnside. Here we examine data from the MFI (Magnetic Fields Investigation, dual triaxial fluxgate magnetometer array) [*Lepping et al.*, 1995] and SWE (Solar Wind Experiment, measuring plasma velocity, density, temperature and electron heat flux) instruments [*Ogilvie et al.*, 1995].

[18] Let us now turn our attention to Figure 3, which reveals the fields and plasma data from Wind from a period

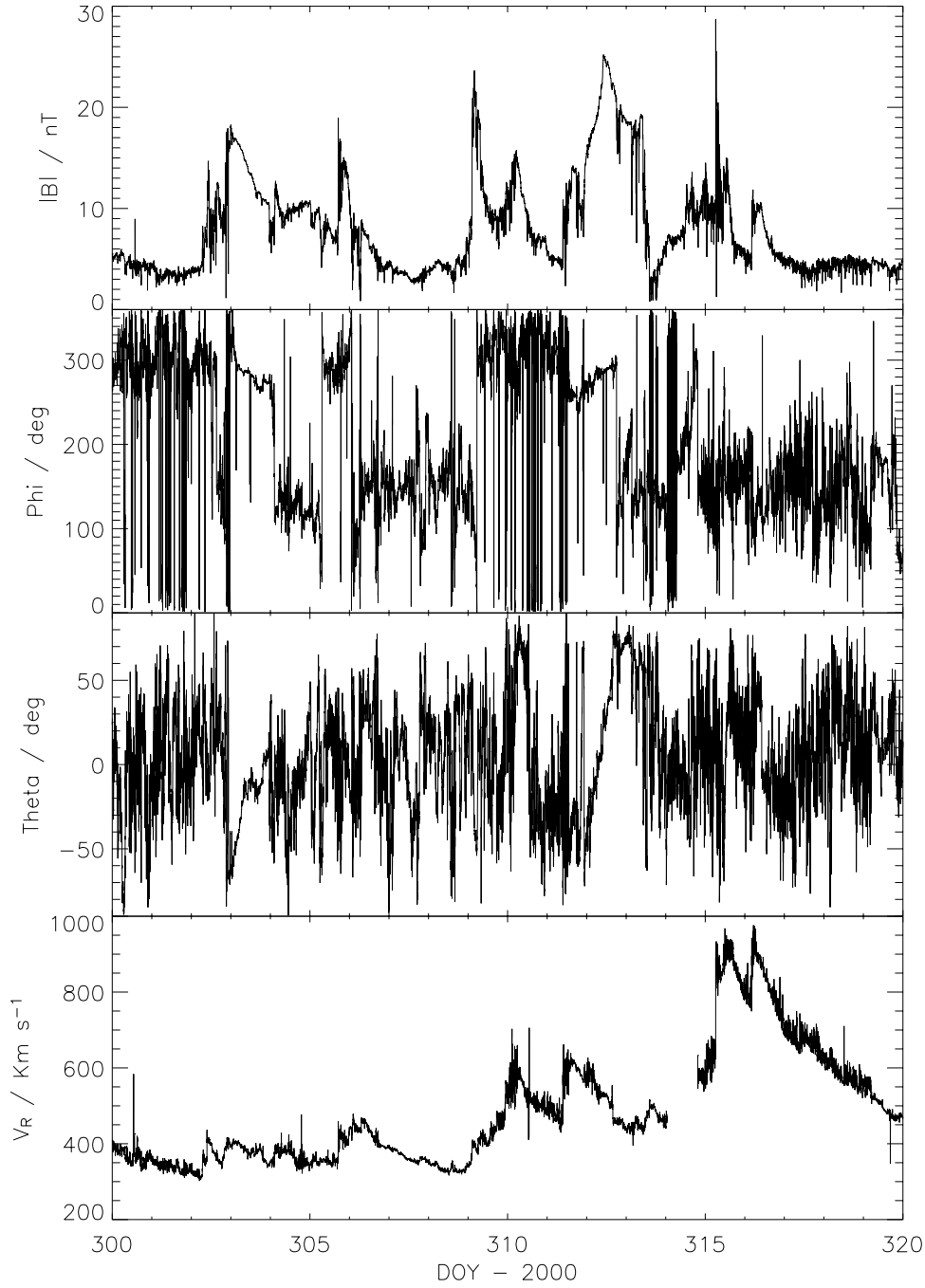

Figure 3. Data taken by the Wind spacecraft at approximately 1 AU showing the IMF magnitude, the φ and θ angles (defined in text), and the (antisunward) solar wind velocity (magnetic field data shown at high resolution to highlight low variance field rotations). The data gap in the bottom panel was due to an extreme flux of solar energetic particles (SEPs) that was measured coincidently by the Large-Angle Spectrometric Coronograph (LASCO) instrument aboard the Solar and Heliospheric Observatory (SOHO) spacecraft.

beginning some 20 days prior to the event observed by Cassini. The top panel, showing magnetic field magnitude, indicates an ambient background field of approximately 5 nT with many enhanced transient events increasing the magnitude to values as high as 25 nT. We note that the velocity of the latter transients (DOY 310 and 312) was over 600 km s^{-1}, as opposed to that of the ambient 400 km s^{-1} solar wind. The final two events shown in Figure 3 (DOY 315 and 316) reached well over 900 km s^{-1}. The second panel shows the φ angle (defined above), with the characteristic discontinuities as the HCS convects over the spacecraft clearly revealed.

[19] As the MFI data in Figure 3 has been plotted at high resolution, two of the transient enhancements observed in the field magnitude data (DOY 303 and DOY 312) can be seen to correspond to low variance intervals in the θ (third

panel) and φ angles. Further inspection reveals that significant field rotations are occurring in both angles. These are classic examples of the signatures observed in interplanetary magnetic field data as a flux rope convects past the spacecraft. Although not shown for simplicity, the other plasma parameters are all consistent with the conclusion that these events are magnetic clouds; there is a decrease in proton temperature coinciding with the field rotation, as well as an enhancement in the He^{++}/p^{+} ratio. There is also a pile-up region preceding the event, characterized by raised field magnitude, proton density, and temperature. Henceforth, we shall refer to these two events as ICME-1 and ICME-2, respectively.

[20] We will now turn our attention to the event at Wind starting on DOY 315, in which a quite different structure is observed. A point to note is the gap in the plasma data prior to the event; this was due to a Sun sensor aboard the spacecraft being unable to operate due to a high intensity of solar energetic particles (SEPs). These particles often stream along the IMF field lines as a precursor to transient solar wind events. Although the SWE instrument took data during this period, the standard data processing routines were unable to produce bulk plasma moments because of this sensor failure. During this period, SEPs were observed coincidentally as a "snowstorm" event by the Large-Angle Spectrometric Coronograph (LASCO) instrument aboard the Solar and Heliospheric Observatory (SOHO) spacecraft (available at http://lasco-www.nrl.navy.mil/cmelist.html). No significant sudden changes in the plasma parameters were observed during this period (A. J. Lazarus, private communication, 2003). A few hours after SWE resumed taking data, the magnetometers observed an enhancement in the field peaking at 25 nT. No flux rope can be seen in the magnetic field angles for this event. The plasma velocity at the start of DOY 315 was holding at a steady value of $\sim$600 km s^{-1}. At 0600 UT the velocity increased to over 900 km s^{-1}, then slowly decreased until 0400 UT on DOY 316, where it reached a peak at almost 1000 km s^{-1}. These increases in velocity also correspond to rises in proton temperature, density, and magnetic field. We interpret these events to be ICME driven shock waves, as there are no other events with this range of parameters at this distance from the Sun [*Neugebauer and Goldstein*, 1997]. We will refer to these events henceforth as the ICMEs 3 and 4. These ICMEs have also been identified recently by *Cane and Richardson* [2003].

[21] Let us now turn our attention to the velocities of the aforementioned ICMEs. Inspection of Figure 3 gives approximate values of 400, 575, 900, and 950 km s^{-1} for the top speeds in the R direction of events ICMEs 1–4, respectively. Evidently, a positive gradient exists in the peak velocities observed for each structure. We would expect therefore for the latter events to "catch up" with the former as they travel from 1 to 5 AU, compressing the material and fields in between.

[22] The combination of these speeds with the distance between the positions of the Wind and Cassini spacecraft results in a lag time that is comparable with the time difference between these two observations. In addition, as mentioned above, the angular separation between the two observations was within a few tens of degrees. CMEs observed emerging from the Sun are known to have an average (median) angular width of 72 degrees (50 degrees) [*St Cyr et al.*, 2000], much wider than the separation between Wind and Cassini. On the assumption that the two observations are linked, we use the limited observations we have available from the Cassini plasma instrument for this period (bottom panel, Figure 2) to infer the speeds of these events at 5 AU and hence some average transit speed. Owing to the apparent increase in velocity throughout the Cassini data set we assign increasing final velocities through ICMEs 1–4. Assuming speeds at Cassini of 400 and 525 km s^{-1} for ICME-1 and ICME-2 and 580 km s^{-1} for ICMEs 3 and 4 and a total distance of $5.65-5.69 \times 10^{8}$ km (owing to Cassini approaching Jupiter throughout the data set), we obtain transit times of approximately 16.3, 11.9, 8.9, and 8.6 days. This gives approximate arrival dates of 319.3, 323.4, 324.2, and 324.8, respectively (using a straight average of the velocities of each event at 1 and 5 AU).

[23] Turning our attention back to Figure 1, we can see that this would suggest that ICME-1 arrives at a time when we have rather a large data gap. The other events however seem to have coalesced into one overall structure, this being the DOY 323–328 Cassini event. No subsequent major events were seen at Wind for 2 weeks, adding weight to our conclusion that we are indeed correlating associated structures.

[24] Frozen-in field discontinuities associated with the traversal of the HCS will be carried out radially with the solar wind as it convects antisunward. We can compare the field polarity (φ-angle) at Wind and Cassini (see Figures 2 and 3) for these two periods and should observe very similar signatures at both spacecraft. As we might expect, there are differences between the two (owing to both the small longitudinal separation between the two observations and perturbations to the HCS structure by these transient events), but both share a similar polarity reversal (from $\sim$300° to $\sim$120°) during the periods in question (DOY 312 at Wind). We can plainly associate this polarity reversal at Wind with the magnetic cloud of ICME-2. This is consistent with the theory that ICMEs can replace the HCS [*Crooker et al.*, 1998]. At Cassini we see an equivalent polarity reversal arrive at approximately the point in time that we expect from our crude ballistic projections (DOY 324). However, the magnetic cloud at the sector boundary that was so plainly visible in the Wind data set is not at all as apparent at Cassini. There are many interesting magnetic field rotations throughout the DOY 323 event observed by Cassini, for example the large rotation in the θ angle on DOY 325. This rotation however is in almost completely the opposite sense to that observed within the DOY 312 magnetic cloud at Wind. In addition, there is a large drop in the field magnitude approximately half way through this rotation. As stated above, one of the defining characteristics of an MC is an overall increase in the field magnitude throughout the duration of the field rotation.

[25] These data suggest then that either (or more probably a combination) of two scenarios has occurred. Either the small longitudinal separation between the two spacecraft has provided us with observations from significantly different regions within the ICME, that we are seeing a "cut" at Cassini that passes through a far different region of the structure. Alternatively, the magnetic cloud that was observed at Wind could have been very substantially

deformed and/or rotated as a consequence of the compression acted upon it by the extremely fast streams behind it. In addition, the MC may have been wholly or partly dissipated through magnetic reconnection during transit.

[26] Counterstreaming electrons were observed during the passage of the Cassini DOY 323 event by the Cassini CAPS ELS (Electron Spectrometer) instrument (A. Rymer, private communication, 2002). Counterstreaming electrons are often associated with ICMEs due to their large-scale loop-like structure being anchored at both ends to the solar surface. This provides further substantiation of the ICME nature of the DOY 323 event at Cassini.

4. MHD Propagation

4.1. Confirmation of Ballistic Projection

[27] In order to test the validity of using such ballistic projections to map solar wind phenomena between distant but radially aligned points within the heliosphere, we have used a one-dimensional MHD projection of data taken near the Earth. The data used to perform this simulation were taken from the Dual Technique Magnetometer (MAG) [*Smith et al.*, 1998] and Solar Wind Electron Proton Alpha Monitor (SWEPAM) [*McComas et al.*, 1998] instruments aboard the Advanced Composition Explorer (ACE) spacecraft [*Stone et al.*, 1998]. The code used to solve the MHD equations was the Versatile Advection Code (VAC) [*Tóth*, 1996].

[28] There are many subtle difficulties in performing these projections, such as the constraining nature of $\nabla \cdot \mathbf{B} = 0$, which forces the radial component of the magnetic field to fall off as exactly one over the radius squared as the plasma travels antisunward. Also, the difference in angle between the two points of observation adds additional complications to the interpretation of the results of such one-dimensional simulations.

[29] Figure 4 shows a stacked plot of the magnetic field magnitude outputted from this model for the period in between DOY 309 and 322 of the year 2000. The horizontal axis of the plot ranges from 1 to 5.5 AU, with time increasing from the top to the bottom of the stack. The temporal evolution of the magnetic field magnitude in the solar wind can therefore be seen as we look down the figure from the top. The coalescence of multiple events into an MIR can be clearly seen on the figure, with large separate field perturbations being introduced at 1AU (on the left side of the figure) on DOY 309 and 313, as is evident in the Wind data in Figure 3. These events subsequently merge to become the single overall event that can be clearly seen on DOY 322, the very bottom trace on the figure. This MIR event appears to stretch from almost 3 to 5 AU, with a raised magnitude ''interaction region'' in the center where compression has taken place. The results of Figure 4 confirm the conclusions regarding the merged interaction region that we arrived at using simple ballistic projections. We will compare the accuracy of the arrival times predicted by both the MHD model and the ballistic projections against the Cassini data below.

4.2. Accuracy of the Model

[30] By inverting the way in which we view the results of this MHD model, we can extract a predicted time series at any chosen radial range. This can then be compared with actual data taken by Cassini in order to test the accuracy of the MHD propagation. Figure 5 shows for comparison the magnetic field magnitude, the φ angle (defined above), the velocity, density, and dynamic pressure (ρv^2) of the solar wind as measured by Cassini on its Jupiter approach (lighter traces) and that predicted by the model (darker traces). Marked on all panels is the point in the time series (late on DOY 335) where the Earth and Jupiter were at the same geometric heliospheric longitude. When considering ''opposition,'' however, we must take into account the transit time of material between the planets. The plasma that we measure at Earth at opposition will not reach 5 AU until 13–17 days later, when Jupiter has moved away from geometrical opposition. So we must define an ''apparent opposition'' (AO), which takes account of this transit time. This will therefore occur around DOY 337.

[31] Figure 5 has been plotted so that data are shown 20–25 days (or degrees, as the Earth and Jupiter move at a relative angular velocity of very close to 1 degree per day) either side of AO. As can be seen, the correlation between the model and the data is remarkably good for the DOY 323 event (the structure we interpret to be an MIR). The model predicts the arrival time of the event at almost exactly DOY 323.0; this is 0.7 days too early, an error of approximately 6% of the overall transit time from 1 AU. The ballistic projection, however, predicted an arrival time of 323.4, less than half the error of the numerical simulation. The model also predicts the magnetic field magnitude profile of the DOY 323 structure rather well in a qualitative sense. There is an overall raised magnitude throughout the event

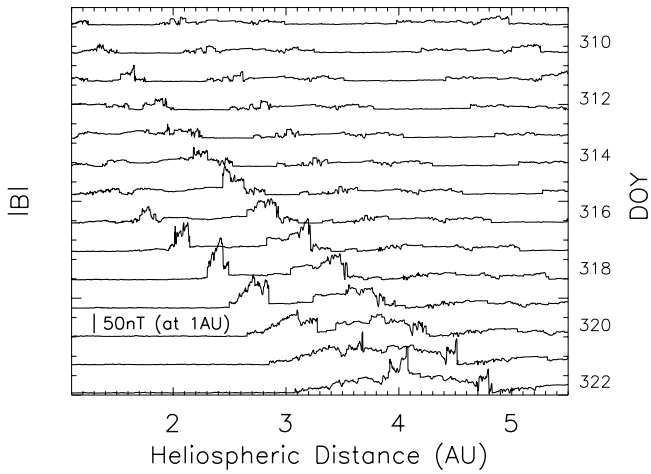

Figure 4. This figure shows the output of a one-dimensional MHD model in which solar wind parameters measured near the Earth have been allowed to propagate radially outward throughout the heliosphere. The magnetic field magnitude has been normalized to its value at 1 AU and has been plotted between 1 and 5.5 AU; the scale shown therefore is only valid at 1 AU. The output of the model has been obtained each day between DOY 2000-309 and 2000-322 and the results stacked vertically. The temporal evolution of the magnetic field in the solar wind can therefore be seen as we look down the figure from the top.

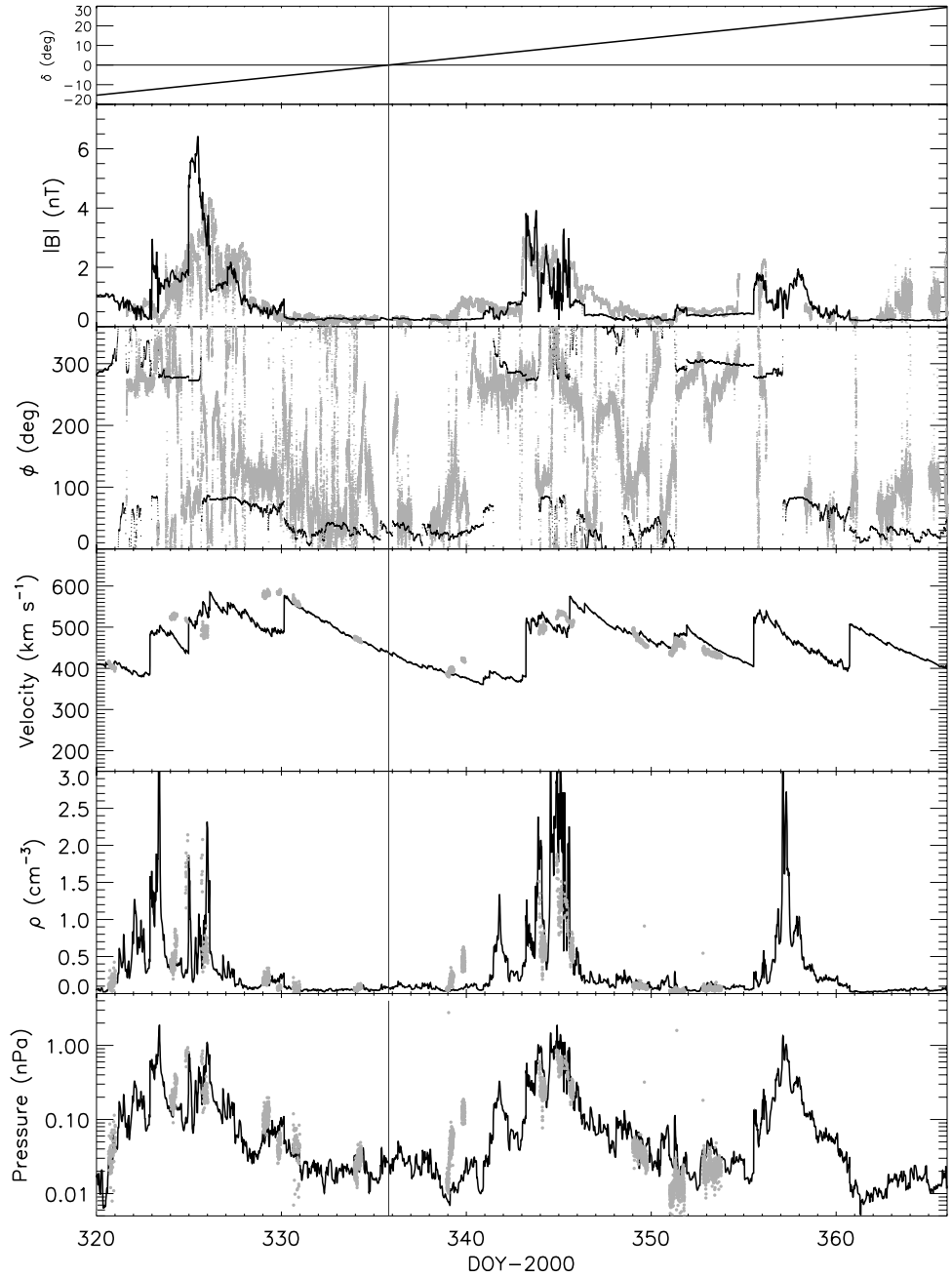

Figure 5. The upper panel shows the difference in heliospheric longitude between the Earth and Cassini (δ), measured in degrees. The remaining panels show respectively the solar wind magnetic field magnitude, φ angle (defined in text), velocity, density, and dynamic pressure (ρv^2) as measured by the Cassini MAG and CAPS instruments (lighter trace) as the spacecraft approached Jupiter. The darker traces show the same properties predicted by a one-dimensional MHD propagation of the solar wind projected from Earth. The large data gaps seen in the plasma data are due to the instrument being unable to view in the solar wind flow direction due to scheduled remote sensing observations.

with a much higher-magnitude central "interaction region." However, the model overestimates the magnitude of this central compressed region. As can be seen, the predicted crossing of the HCS (the discontinuity in the φ angle halfway though DOY 325) also arrives close to the observed crossing within the data. Apart from a rather disturbed period (DOY 345–350), the φ polarity remains very well predicted by the model for the whole of the data set plotted on Figure 5. An accuracy of on the order of plus or minus 1 day in the arrival time of the polarity reversals is observed.

[32] Shown in Figure 5, along with the DOY 323 event, are two other large field perturbations (DOY 343 and 354). By using ballistic estimates similar to those above and by inspection of plots similar to Figure 4 (not shown), we are able to confidently associate the structure observed by Cassini on DOY 343 with the ICME observed near the Earth on DOY 332 [*Cane and Richardson*, 2003]. The

magnetic magnitude profile of this event is also predicted well by the model. The final structure plotted on Figure 5 (DOY 354) appears to map back to an increase in solar wind velocity observed by the ACE spacecraft on DOY 343. No ICME is recorded by *Cane and Richardson* [2003] for this event.

[33] From the comparison between the MAG data plotted in Figure 5 and that predicted by the MHD propagation, it would seem that the model predicts the magnetic structure of the solar wind to an impressive degree, albeit with an arrival time accuracy of approximately plus or minus 1 day. The predicted plasma parameters plotted in Figure 5 (density, velocity, and dynamic pressure) are also in good agreement with the data. A complete comparison between the model and the plasma data is rendered difficult due to the large data gaps (owing to pointing restrictions imposed on the instrument, as mentioned above). However, for periods where data are available, we can see that within the ''events'' plotted, the model predicts substantial increases in the dynamic pressure. This is to be expected within compressional solar wind structures such as ICME driven shock waves and Corotating Interaction Regions (CIRs) and is confirmed by the available data. The solar wind dynamic pressure is a parameter of great interest when considering ''space weather'' at Jupiter. Recent theoretical modeling of the Jovian magnetosphere-ionosphere (MI) coupling system suggests that it is predominantly the solar wind dynamic pressure (rather than the strength of Bz, as at the Earth) that is the major driving factor in modulating MI current intensity throughout the Jovian middle magnetosphere (and hence main auroral oval emission) [*Southwood and Kivelson*, 2001; *Cowley and Bunce*, 2001].

[34] Farther away from AO, as the planets become less aligned, the model copes less well (not shown). This is unsurprising as we are projecting data measured in one angular sector of the heliosphere and then comparing this to data taken in another sector. Past DOY 363 the model deviates from the data as the spacecraft is no longer in the solar wind and has entered the Jovian magnetosheath (Dougherty et al., submitted manuscript, 2004), where an extremely extended period of mirror mode instabilities was observed [*Andre et al.*, 2002].

5. Summary

[35] Observations of transient solar wind streams in the Cassini upstream magnetometer data from the period prior to Jupiter closest approach have been presented. One of these events is examined and by simple ballistic projection is found to be a merged interaction region. This structure was formed from the coalescence of a magnetic cloud and two unusually fast solar wind streams that were observed far upstream near Earth, which was fortuitously within the same angular sector of the heliosphere. Comparable magnetic field rotations associated with the magnetic cloud that was observed by Wind are not apparent in the Cassini data. This suggests that it has either been missed due to the small longitudinal separation between the two observations, compressed beyond recognition, or has been dissipated through some other process such as magnetic reconnection.

[36] Previous investigations into the formation of MIRs from ICMEs [e.g., *Richardson et al.*, 2002] have focused on the large scale, tying together a string of interconnected (if highly longitudinally separated) observations from the Sun to the outer heliosphere. Examination of the evolution of the detailed internal structure of such solar wind events over large heliospheric distances requires that at least two spacecraft be within a few degrees of the same radial vector from the Sun. The occurrence of such an alignment is infrequent and almost always by chance. Although the angular separation between the two observations outlined here is less than 20 degrees, this is not sufficient to make solid statements regarding the evolution of the magnetic cloud that is swept up into the DOY 323 event at Cassini. However, these observations do pose interesting questions regarding the fate of flux-rope structures that become involved in compression regions within the solar wind. A full three-dimensional MHD simulation of this type of interaction would be required in order to understand the phenomenon more fully [e.g., *Schmidt and Cargill*, 2003]. Magnetic clouds are observed at Ulysses at these heliospheric distances [*Rees and Forsyth*, 2003].

[37] The conclusions arrived at using ballistic projections have been tested successfully by employing a one-dimensional MHD propagation of the solar wind from data taken at 1 AU. The output of this model was then compared with the magnetic field and plasma data taken by Cassini in order to test its accuracy. It was found that as expected, the model coped best closest to opposition, when the two points of observation were more radially aligned. In general the model is found to predict the large-scale structure of the solar wind to an accuracy of plus or minus 1 day in arrival time approximately 20–25 degrees either side of (apparent) opposition. Examination of Figure 5 reveals that the typical duration of the transient structures within this data set is 5–10 days. We conclude therefore that for use in comparisons with large-scale variations in Jovian magnetospheric behavior, this MHD model can provide a very useful insight into the external drivers that may be producing observed behaviour within the system; indeed this is what has been undertaken in a companion paper that accompanies this publication [*Hanlon et al.*, 2004].

[38] As the Earth and Jupiter pass one another longitudinally approximately once every 13 months, we plan to perform similar projections for the last 8 years. This will provide seven periods of quasi-solar wind data, which can be then compared with any signatures of interest within the Galileo data set. This will be the subject of future work.

[39] **Acknowledgments.** PGH wished to thank the PI of the Wind MFI instrument, R. P. Lepping, the PI of the Wind SWE instrument, K. W. Ogilvie, the PI of the ACE MAG instrument, C. W. Smith, and the PI of the ACE SWEPAM instrument, D. J. McComas. We also thank the LASCO operations scientists for compiling the preliminary CME catalogues. SOHO is a project of international cooperation between ESA and NASA. PGH also wishes to thank J. P. Eastwood and A. Rees for insightful discussions. PGH was supported for the duration of this work by a UK PPARC quota studentship. GT has been supported by the Hungarian Science Foundation (OTKA grant T037548). FJC has been supported by NASA/JPL through JPL contract 1243218.

[40] Arthur Richmond thanks Marcia Neugebauer and another reviewer for their assistance in evaluating this paper.

References

Andre, N., G. Erdos, and M. K. Dougherty (2002), Overview of mirror mode fluctuations in the Jovian dusk magnetosheath: Cassini magnetometer observations, *Geophys. Res. Lett.*, *29*(20), 1980, doi:10.1029/2002GL015187.

Borrini, G., J. T. Gosling, S. J. Bame, and W. C. Feldman (1982), Helium abundance enhancements in the solar wind, *J. Geophys. Res.*, *87*(A9), 7370–7378.

Burlaga, L. F. (1995), Merged interaction regions, in *Interplanetary Magnetohydrodynamics*, *Int. Ser. on Astron. and Astrophys.*, pp. 138–165, Oxford Univ. Press, New York.

Burlaga, L. F. (1998), Magnetic clouds and force-free fields with constant-alpha, *J. Geophys. Res.*, *93*(A7), 7217–7224.

Burlaga, L. F., and N. F. Ness (1993), Large-scale distant heliospheric magnetic field: Voyager 1 and 2 observations from 1986 through 1989, *J. Geophys. Res.*, *98*(A10), 17,451–17,460.

Burlaga, L. F., E. Sittler, F. Mariani, and R. Schwenn (1981), Magnetic loop behind an interplanetary shock: Voyager, Helios, and IMP-8 observations, *J. Geophys. Res.*, *86*(A8), 6673–6684.

Cane, H. V., and I. G. Richardson (2003), Interplanetary coronal mass ejections in the near-Earth solar wind during 1996–2002, *J. Geophys. Res.*, *108*(A4), 1156, doi:10.1029/2002JA009817.

Cargill, P. J. (2001), Coronal mass ejections at the Sun and in interplanetary space, in *NATO ASI Space Storms and Space Weather Hazards*, p. 177, Kluwer Acad., Norwell, Mass.

Clarke, J. T., et al. (2002), Ultraviolet emissions from the magnetic footprints of Io, Ganymede and Europa on Jupiter, *Nature*, *415*(6875), 997–1000.

Cowley, S. W. H., and E. J. Bunce (2001), Origin of the main auroral oval in Jupiter's coupled magnetosphere-ionosphere system, *Planet. Space Sci.*, *49*, 1067–1088.

Crooker, N. U., J. T. Gosling, and S. W. Kahler (1998), Magnetic clouds at sector boundaries, *J. Geophys. Res.*, *103*(A1), 301–306.

Dougherty, M. K., et al. (2004), The Cassini magnetic field investigation, *Space Sci. Rev.*, in press.

Gopalswamy, N., A. Lara, S. Yashiro, M. L. Kaiser, and R. A. Howard (2001), Predicting the 1-AU arrival times of coronal mass ejections, *J. Geophys. Res.*, *106*(A12), 29,207–29,217.

Gosling, J. T. (1990), Coronal mass ejections and magnetic flux ropes in interplanetary space, in *Physics of Magnetic Flux Ropes*, *Geophys. Monogr. Ser.*, vol. 58, edited by C. T. Russell et al., AGU, Washington, D.C.

Gosling, J. T., V. Pizzo, and S. J. Bame (1973), Anomalously low proton temperatures in the solar wind following interplanetary shocks: Evidence for magnetic bottles?, *J. Geophys. Res.*, *78*, 2001.

Gurnett, D. A., W. S. Kurth, R. R. Shaw, A. Roux, R. Gendrin, C. F. Kennel, F. L. Scarf, and S. D. Shawhan (1992), The Galileo Plasma-Wave investigation, *Space Sci. Rev.*, *60*(1–4), 341–355.

Gurnett, D. A., et al. (2002), Control of Jupiter's radio emission and aurorae by the solar wind, *Nature*, *415*, 985–987.

Gurnett, D. A., et al. (2004), The Cassini radio and plasma wave science investigation, *Space Sci. Rev.*, in press.

Hanlon, P. G., M. K. Dougherty, N. Krupp, K. C. Hansen, F. J. Crary, D. T. Young, and G. Tóth (2004), Dual spacecraft observations of a compression event within the Jovian magnetosphere: Signatures of externally triggered super-corotation?, *J. Geophys. Res.*, *109*, A09S09, doi:10.1029/2003JA010116.

Henke, T., J. Woch, R. Schwenn, U. Mall, G. Gloeckler, R. von Steiger, R. J. Forsyth, and A. Balogh (2001), Ionization state and magnetic topology of coronal mass ejections, *J. Geophys. Res.*, *106*(A6), 10,597–10,613.

Hundhausen, A. J. (1993), Sizes and locations of coronal mass ejections: SMM observations from 1980 and 1984–1989, *J. Geophys. Res.*, *98*(A8), 13,177–13,200.

Klein, L. W., and L. F. Burlaga (1982), Interplanetary magnetic clouds at 1 AU, *J. Geophys. Res.*, *87*(A2), 613–624.

Lepping, R. P., J. A. Jones, and L. F. Burlaga (1990), Magnetic field structure of interplanetary magnetic clouds at 1 AU, *J. Geophys. Res.*, *95*(A8), 11,957–11,965.

Lepping, R. P., et al. (1995), The Wind magnetic field investigation, *Space Sci. Rev.*, *71*, 207.

Lepri, S. T., T. H. Zurbuchen, L. A. Fisk, I. G. Richardson, H. V. Cane, and G. Gloeckler (2001), Iron charge distribution as an identifier of interplanetary coronal mass ejections, *J. Geophys. Res.*, *106*, 29,231.

McComas, D. J., S. J. Bame, S. J. Barker, W. C. Feldman, J. L. Phillips, P. Riley, and J. W. Griffee (1998), Solar wind electron proton alpha monitor (SWEPAM) for the advanced composition explorer, *Space Sci. Rev.*, *86*, 563–612.

Neugebauer, M., and R. Goldstein (1997), Particle and field signatures of coronal mass ejections in the solar wind, in *Coronal Mass Ejections*, *Geophys. Monogr. Ser.*, vol. 99, edited by N. Crooker, J. A. Joselyn, and J. Feynman, pp. 245, AGU, Washington, D.C.

Ogilvie, K. W., et al. (1995), SWE, a comprehensive plasma instrument for the Wind spacecraft, *Space Sci. Rev.*, *71*, 55–77.

Paularena, K. I., C. Wang, R. von Steiger, and B. Heber (2001), An ICME observed by Voyager 2 at 58 AU and by Ulysses at 5 AU, *Geophys. Res. Lett.*, *28*(14), 2755–2758.

Prangé, R., and L. Pallier (2002), Morphology and dynamics of Saturn's FUV aurora, paper presented at the Magnetospheres of the Outer Planets Conference, Appl. Phys. Lab., Johns Hopkins Univ., Laurel, Md.

Rees, A., and R. J. Forsyth (2003), Magnetic clouds with east/west orientated axes observed by Ulysses during solar cycle 23, *Geophys. Res. Lett.*, *30*(19), 8030 doi:10.1029/2003GL017296.

Richardson, J. G., and H. V. Cane (1995), Regions of abnormally low proton temperature in the solar wind (1965–1991) and their association with ejecta, *J. Geophys. Res.*, *100*(A12), 23,397–23,412.

Richardson, J. D., K. I. Paularena, C. Wang, and L. F. Burlaga (2002), The life of a CME and the development of a MIR: from the Sun to 58 AU, *J. Geophys. Res.*, *107*(A4), 1041, doi:10.1029/2001JA000175.

Schmidt, J. M., and P. J. Cargill (2003), Magnetic reconnection between a magnetic cloud and the solar wind magnetic field, *J.Geophys. Res.*, *108*(A1), 1023, doi:10.1029/2002JA009325.

Smith, C. W., J. L. Heureux, N. F. Ness, M. H. Acuna, L. F. Burlaga, and J. Scheifele (1998), The ACE magnetic experiment, *Space Sci. Rev.*, *86*, 613–632.

Southwood, D. J., and M. G. Kivelson (2001), A new perspective concerning the influence of the solar wind on the Jovian magnetosphere, *J. Geophys. Res.*, *106*, 6123–6130.

Stone, E. C., A. M. Frandsen, R. A. Mewaldt, E. R. Christian, D. Margolies, J. F. Ormes, and F. Snow (1998), The advanced composition explorer, *Space Sci. Rev.*, *86*, 1–22.

St Cyr, O. C., et al. (2000), Properties of coronal mass ejections: SOHO LASCO observations from January 1996 to June 1998, *J. Geophys Res.*, *105*(A8), 18,169–18,185.

Tóth, G. (1996), A general code for modeling MHD flows on parallel computers: Versatile Advection Code, *Astrophys. Lett. Comms.*, *34*, 245.

Wang, C., J. D. Richardson, and L. Burlaga (2001), Propagation of the Bastille Day 2 000 CME shock in the outer heliosphere, *Solar Phys.*, *204*, 411–421.

Young, D. T., et al. (2004), Cassini plasma spectrometer investigation, *Space Sci. Rev.*, in press.

F. J. Crary and D. T. Young, Southwest Research Institute, San Antonio, TX 78228-0510, USA. (fcrary@swri.edu; dyoung@swri.edu)

M. K. Dougherty, R. J. Forsyth, P. G. Hanlon, and M. J. Owens, Space and Atmospheric Physics Group, Blackett Laboratory, Imperial College London, London SW7 2BW, UK. (m.dougherty@imperial.ac.uk; r.forsyth@imperial.ac.uk; paul.hanlon@imperial.ac.uk; mathew.owens@imperial.ac.uk)

K. C. Hansen, Department of Atmospheric, Oceanic, and Space Sciences, University of Michigan, Ann Arbor, MI 48109, USA. (kenhan@umich.edu)

G. Tóth, Department of Atomic Physics, Loránd Eötvös University, 1117 Budapest, Hungary. (gtoth@hermes.elte.he)